Chaotic antiphase dynamics and synchronization in multimode semiconductor lasers

A. Uchida,* Y. Liu, I. Fischer,† P. Davis, and T. Aida
ATR Adaptive Communications Research Laboratory, 2-2 Hikaridai, Seika-cho, Soraku-gun, Kyoto 619-0288, Japan
(Received 21 August 2000; revised manuscript received 2 February 2001; published 28 June 2001)

We report experimental observation of antiphase mode dynamics in the high-frequency chaotic state of a multimode semiconductor laser with optical feedback and provide a detailed investigation of its frequency dependence. Comparison of the power spectral density for total intensity with the incoherent sum of power spectral densities for individual mode intensities shows that the oscillations around the relaxation oscillation frequency are in-phase in all the modes, while the oscillations at lower frequencies exhibit partial antiphase behavior. We demonstrate that synchronized phase dynamics with similar frequency dependence can be induced in a second laser by unidirectional optical injection.

DOI: 10.1103/PhysRevA.64.023801 PACS number(s): 42.65.Sf, 42.55.Px, 05.45.Xt

I. INTRODUCTION

The dynamics of chaotic multimode semiconductor lasers is currently of considerable interest from the viewpoints of both fundamental physics and applications. Experimental observations and numerical simulations have been reported which show that multimode dynamics can play a significant role in a variety of complex dynamical phenomena, including low-frequency fluctuations (LFF) and high-frequency chaotic oscillations [1–6]. Also, the synchronization of multimode dynamics in lasers has been considered as a mechanism for multiwavelength transmission of encoded data [7–9].

A key issue in the behavior of multimode lasers is how the oscillations of different modes are related to each other. One general behavior that has been observed in multimode lasers is antiphase dynamics [10–17]. Antiphase is a property related to coherence of the phases of the oscillations of the mode intensities rather than the optical phases. Alternating pulsations in two modes due to mode coupling is a simple example of antiphase dynamics. Antiphase dynamics have been shown to occur in the relaxation in a multimode class-B laser with cross saturation, where the lower-frequency components of oscillation of different longtitudinal modes cancel each other completely, so the total laser intensity oscillates with just a single oscillation frequency, resembling the relaxation of a single-mode laser [12,13]. Antiphase dynamics of multilongitudinal modes have been experimentally observed in various laser systems, including microchip lasers [12], solid-state lasers [14,15], fiber lasers [16], and CO_2 lasers [17].

In the case of chaotic semiconductor lasers the nature of mode interaction and antiphase dynamics has not been clear. In class-B lasers, antiphase dynamics has been attributed to cross saturation of modes due to spatial hole burning [10,11]. In semiconductor lasers fast carrier diffusion is expected to suppress spatial hole burning in the longitudinal direction. However, a recent experimental work reported that in the LFF of a multimode semiconductor laser with optical feedback, the recovery of the total laser power was faster than the recovery of individual mode powers, indicating the existence of antiphase dynamics [1]. There was also an observation of a behavior in low-frequency multimode oscillations in which each mode pulse with a repetition rate was dominated by the external cavity round-trip time, but with the phase of pulsation being different for different modes [2]. Antiphase dynamics were shown recently in numerical simulations of LFF behavior in semiconductor laser models with various mechanisms for mode interaction [3–6].

In this paper we give clear experimental evidence of antiphase dynamics in the fast chaotic oscillations in a multimode semiconductor laser and we show the frequency dependence of the antiphase properties. Simultaneous measurement of the total laser intensity and modal intensity is performed to show a direct indication of how the variation of an individual mode relates to the total output. The existence of antiphase behavior for various frequency components is tested by comparing the rf spectra of total intensities with that of the incoherent sum of modal intensities at particular frequencies, following a method of analysis which was conducted in previous studies on class-B lasers [10,11]. We also demonstrate the synchronization of two lasers with antiphase dynamics by coupling these two lasers in a master-slave scheme.

II. OBSERVATION OF CHAOTIC ANTIPHASE DYNAMICS

A. Experimental setup

We investigate antiphase dynamics in fast (up to a few GHz) chaotic oscillations in a semiconductor laser with optical feedback. The laser system is the same as the one used in a recent experiment, in which synchronization of fast chaotic oscillations could be demonstrated [7]. Figure 1 shows our experimental setup. An external mirror is set in front of the laser to provide optical feedback which results in chaotic fluctuation of the laser output. The round-trip time of the light in the external cavity is 3.8 ns, corresponding to a fre-

*Permanent address: Department of Electronics and Systems, Takushoku University, 815-1 Tatemachi, Hachioji, Tokyo, 193-0985, Japan.

†Permanent address: Institute of Applied Physics, Darmstadt University of Technology, Schloßgartenstraße 7, 64289 Darmstadt, Germany.

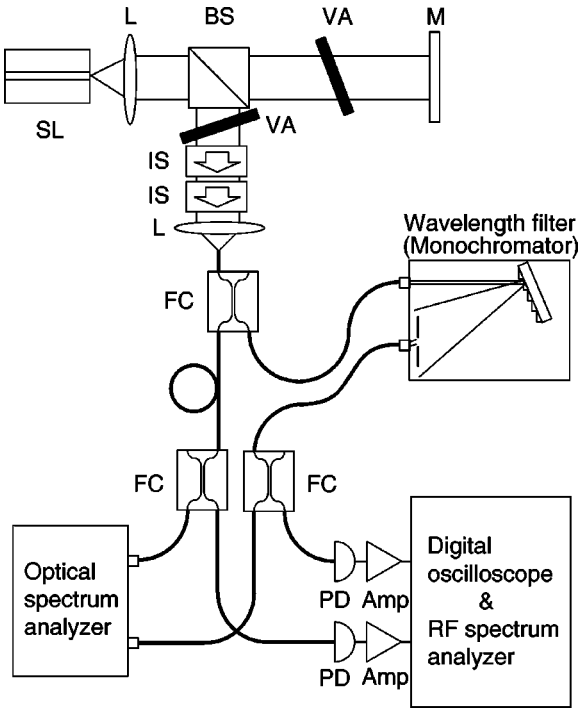

FIG. 1. Experimental setup for observation of antiphase dynamics. SL's: semiconductor lasers; L's: lenses; BS: beam splitter; M: mirror; VA's: variable attenuators; IS's: isolators; FC's: fiber couplers; PD's: photodiodes; Amp's: amplifiers.

quency of 0.265 GHz. A variable attenuator (ND filter) is adjusted to get the appropriate weak optical feedback conditions, so that the laser is in a chaotic state with oscillations of laser intensity output at frequencies up to a few GHz. We used a semiconductor laser (Anritsu SD3F513T) emitting at about 1460 nm. One facet of the laser is antireflection (AR) coated and has only 5% reflectivity. The laser is driven by a low-noise current source (Kette KNN-300LT) and is temperature stabilized with 0.01 K accuracy. The injection current of the semiconductor laser is set to 35.0 mA, which is 1.5 times the threshold value, and the output power is 0.770 mW with optical feedback. The relaxation oscillation frequency under these conditions amounts to ~ 2.4 GHz. The optical spectrum of the laser is measured with an optical spectrum analyzer (Anritsu MS9710C) with a resolution of 0.05 nm, which is sufficient to resolve the longitudinal modes of the semiconductor laser. Figure 2 shows a measured optical spectrum of the semiconductor laser in the chaotic state. It can be seen that the laser has multiple longitudinal modes with mode spacing of 0.35 nm.

To separately observe the dynamics of different sets of modes, a bandwidth-variable optical wavelength filter (Hewlett Packard HP70951A) is used as shown in Fig. 1. We can select one of the longitudinal modes by scanning the center wavelength of the filter with a minimum bandwidth of 0.2 nm which is sufficient to restrict the detected light to a single longitudinal mode of the solitary laser. We also set the center wavelength of the optical band-pass filter to 1460.5 nm and use the bandwidths of 1, 5, and 10 nm, which cover sets of three, ten, and 18 longitudinal laser modes, respectively. The dynamical behavior of the intensity of a specific

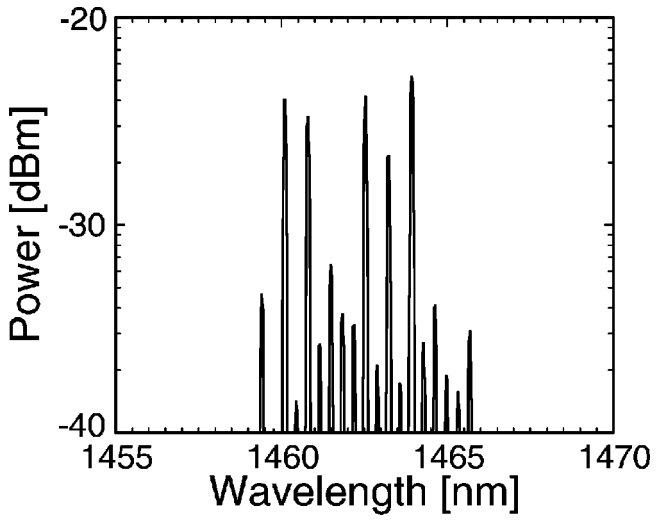

FIG. 2. Optical spectrum of the multilongitudinal-mode semiconductor laser with optical feedback.

mode or mode set is detected with a 6-GHz photodiode (New Focus 1514-LF) and analyzed with a radio-frequency spectrum analyzer (Advantest R3267, 9-GHz bandwidth) and a fast digital oscilloscope (Tektronix TDS694C, 3-GHz bandwidth and 10-G sampling per second).

B. Characterization of multimode RF spectra

With the rf spectrum analyzer we observe the average power spectral densities (PSD) for the total intensity of the selected mode and the corresponding modal intensities. We use the notation $P(I_j,\Omega)$ to represent the amount of PSD at a particular frequency Ω of the rf spectrum of the jth modal intensity I_j, and $P(\Sigma I_j,\Omega)$ to represent the measured PSD for the total intensity of the selected mode sets. We calculate the incoherent sum $\Sigma[P(I_j,\Omega)]$ and the in-phase sum $[\Sigma\sqrt{P(I_j,\Omega)}]^2$ from the measured $P(I_j,\Omega)$. The phase relationship among the oscillations of the modal intensities I_j at a particular frequency Ω can then be calculated as follows [18]: perfect in-phase,

$$P\left(\sum I_j,\Omega\right)=\left(\sum \sqrt{P(I_j,\Omega)}\right)^2, \tag{2.1}$$

partial in-phase,

$$\left(\sum \sqrt{P(I_j,\Omega)}\right)^2 > P\left(\sum I_j,\Omega\right) > \sum [P(I_j,\Omega)], \tag{2.2}$$

partial antiphase,

$$\sum [P(I_j,\Omega)] > P\left(\sum I_j,\Omega\right) > 0, \tag{2.3}$$

and perfect antiphase,

$$P\left(\sum I_j,\Omega\right)=0. \tag{2.4}$$

The value of the incoherent sum $\Sigma[P(I_j,\Omega)]$ is a threshold to distinguish in-phase states, where coherent summation is achieved as a result of constructive summation among N-mode intensities, and antiphase states, where summation is destructive.

C. Observations of antiphase dynamics

We measured PSD of total intensity $P(\Sigma I_j,\Omega)$ (red line), and compared it with PSD of the incoherent sum $\Sigma[P(I_j,\Omega)]$ (blue line), and in-phase sum $[\Sigma\sqrt{P(I_j,\Omega)}]^2$ (green line) for the selected sets of (a) three-mode, (b) ten-mode, and (c) 18-mode dynamics as shown in Fig. 3. The PSDs of total intensity (red line) are typical for feedback-induced chaos [7]. The broad maxima of the spectrum correspond to the round-trip frequency of the light in the external cavity at 0.265 GHz and its harmonics. At the relaxation oscillation frequency Ω_R of $\sim$2.4 GHz, the peak height of the red line is the same as that of the green line for each set of selected modes. This implies that the components of oscillations of the mode intensities at frequencies near Ω_R are perfectly in-phase. On the other hand, the peak height of the red line is clearly lower than that of the blue line in the low-frequency region below 1 GHz. These results imply partial antiphase oscillations of the modes at frequencies lower than the relaxation oscillation frequency Ω_R. As the number of selected modes is increased, the difference between the red line and the blue line becomes larger; that is, the antiphase behavior can be more clearly observed when the number of longitudinal modes increases.

In order to clarify and visualize how these properties manifest itself in the temporal dynamics we have performed direct measurements of the modal intensity dynamics. In the following we present and compare the temporal wave forms of the total intensity with those of the subsets of modes. (Due to experimental limitations, we were unable to simultaneously detect more than one subset of modes.) Figure 4 shows temporal wave forms of (a) one-mode, (b) six-mode, and (c) 15-mode intensities compared with the corresponding total intensities. For one-mode intensity in Fig. 4(a), the amplitude of the chaotic oscillations is small most of the time, and oscillations with high amplitude arise intermittently, so the chaotic temporal wave forms include slow envelope components with oscillation frequency corresponding to the round-trip frequency of the external cavity. As the number of the longitudinal modes is increased, the high amplitude oscillations occur more frequently and the dominant oscillation frequency approaches the relaxation oscillation frequency. Finally, the oscillations for 15 modes are almost identical to those of the total intensity as shown in Fig. 4(c). Thus, the low-frequency component decreases as the number of the mode is increased. On the other hand, in Fig. 4 the phase of the fast relaxation oscillation frequency component is matched between the total and modal intensities regardless of the number of modal intensities. In summary, modal intensities are in-phase around the fast relaxation oscillation frequency components, while, antiphase dynamics is observed for the low-frequency components.

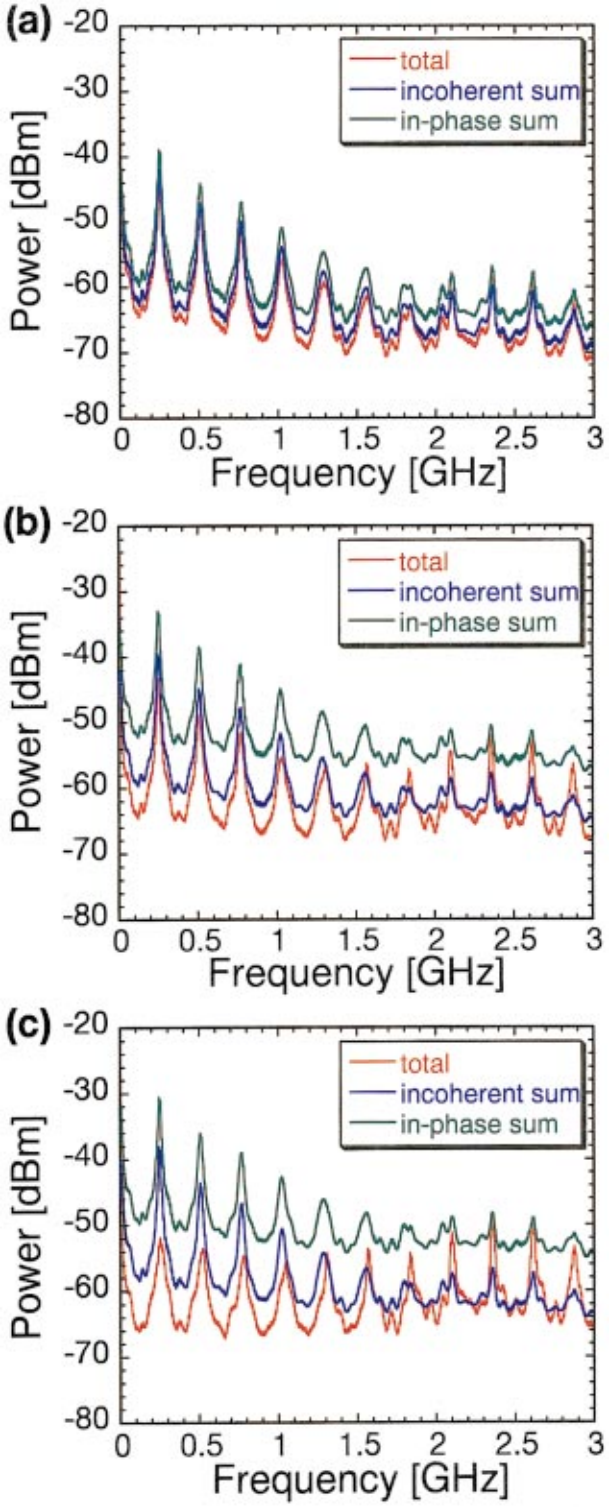

FIG. 3. (Color) Radio-frequency power spectal densities of total intensity $P(\Sigma I_j,\Omega)$ (red line), incoherent sum $\Sigma[P(I_j,\Omega)]$ (blue line), and in-phase sum $[\Sigma\sqrt{P(I_j,\Omega)}]^2$ (green line) at the selected (a) 3-mode, (b) 10-mode, and (c) 18-mode dynamics. Antiphase dynamics is observed at the low-frequency region below 1 GHz and becomes more apparent as the number of the selected modes increases.

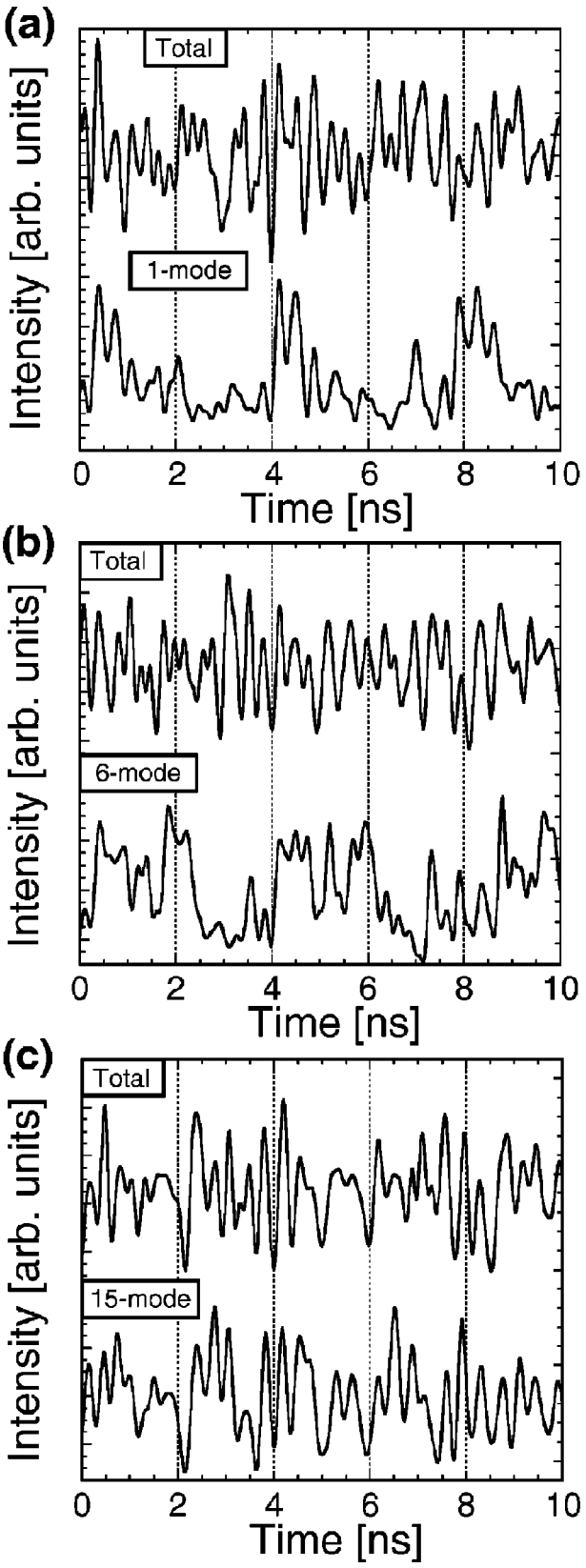

FIG. 4. Temporal wave forms of the selected (a) one-mode, (b) six-mode, and (c) 15-mode intensities compared with the corresponding total intensities. The modal and total intensities were measured simultaneously.

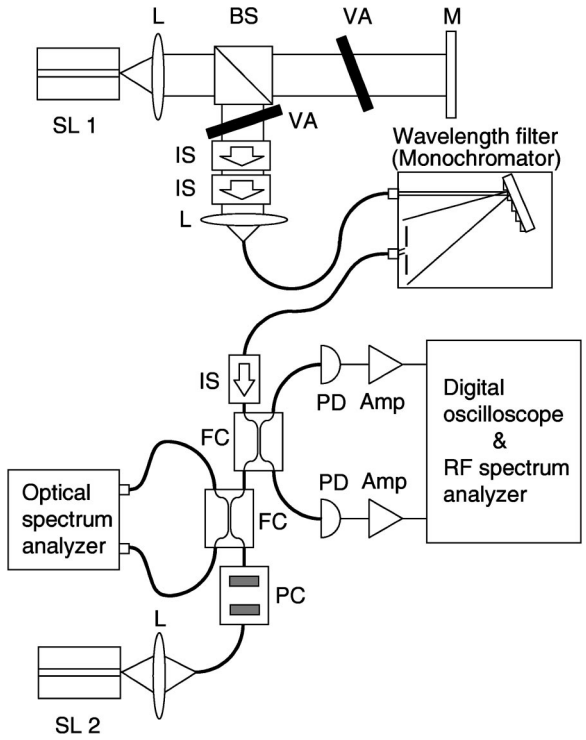

FIG. 5. Experimental setup for observation of synchronization of antiphase dynamics. PC: polarization controller.

D. Discussion

A number of different models of multimode semiconductor lasers have been investigated and shown to exhibit types of antiphase behavior. Viktorov *et al.* introduced carrier gratings due to the spatial hole burning effect in a multimode extension of the Lang-Kobayashi (LK) equations [3]. Rogister *et al.* used multimode LK equations assuming a parabolic gain profile [4]. The self- and cross-saturation effects in multimode LK equations were taken into account in the model of Sukow and co-workers [5]. Huyet *et al.* considered a counterpropagating wave model (without *a priori* mode expansion) for a cavity with a parabolic gain dispersion [6]. All these models have a similar mechanism, gain cross-saturation due to the interaction among modes, and show types of antiphase behavior. According to Refs. [3,4] (Fig. 3 in [3], Fig. 2 in [4]) in the recovery stage of chaotic LFF, the fast pulsing dynamics are in-phase while the frequency components corresponding to variations of pulse heights in the different modes are out of phase, resulting in a reduction in the low-frequency component of the total intensity. In this sense, the behavior of modes during LFF recovery seen in these numerical models is similar to the type of antiphase dynamics observed in our experiment. This supports a conjecture that the existence of a gain cross-saturation among multiple modes could be the key mechanism for the antiphase behavior that we observed. Detailed comparison between models and regimes and types of antiphase dynamics is left for future work.

It should be noted that the distinction between in-phase and antiphase dynamics depends on the frequency of the oscillation components. In Ref. [4], ''in-phase mode dynam-

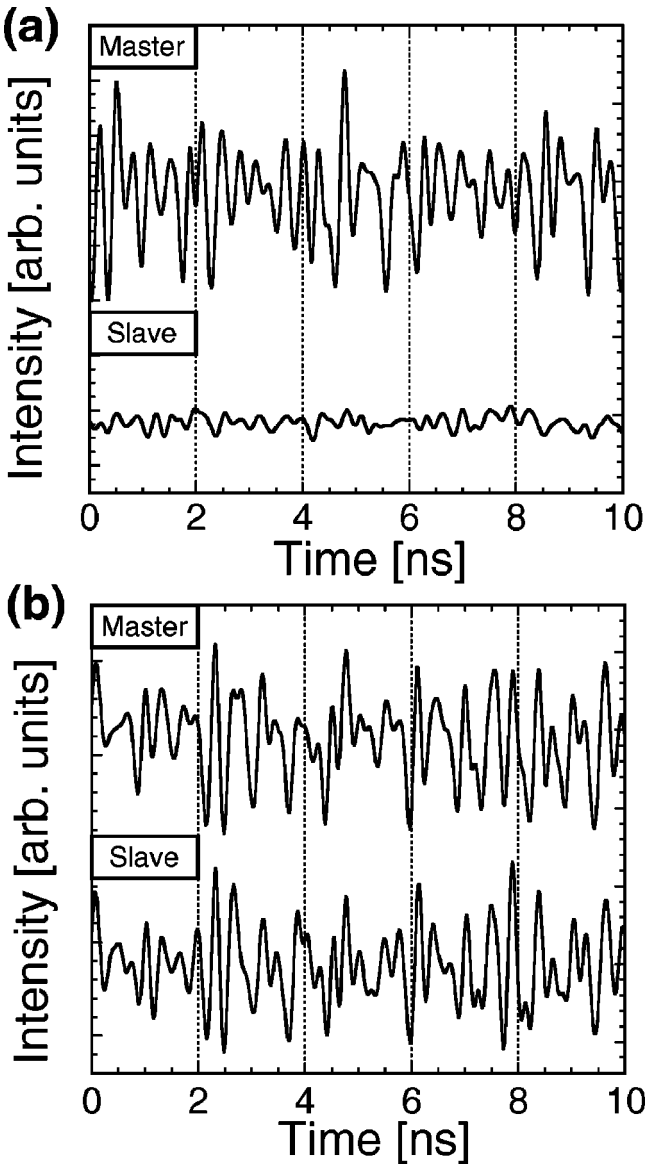

FIG. 6. Temporal wave forms of two laser outputs for total intensity before and after the synchronization. All traces are shown at the same scale.

ics'' corresponds to our observation where in-phase dynamics appear at the relaxation oscillation frequency and antiphase dynamics is also observed at lower-frequency components. On the other hand, in [4] and [6], the term ''antiphase'' has been used for the antiphase relation around the fundamental oscillation frequency in a regime where the total intensity is almost constant. Therefore, it is necessary to indicate both the phase relationship and the corresponding frequency component to determine in-phase and antiphase dynamics.

III. ANTIPHASE DYNAMICS IN SYNCHRONIZED LASERS

Since the total intensity of the multimode dynamics presented here could be synchronized with a second device-identical laser in a recent experiment [7], the question arises of how far the in-phase and antiphase properties of the modal intensities are also transferred from the transmitter to the receiver laser. In this section we demonstrate that synchroni-

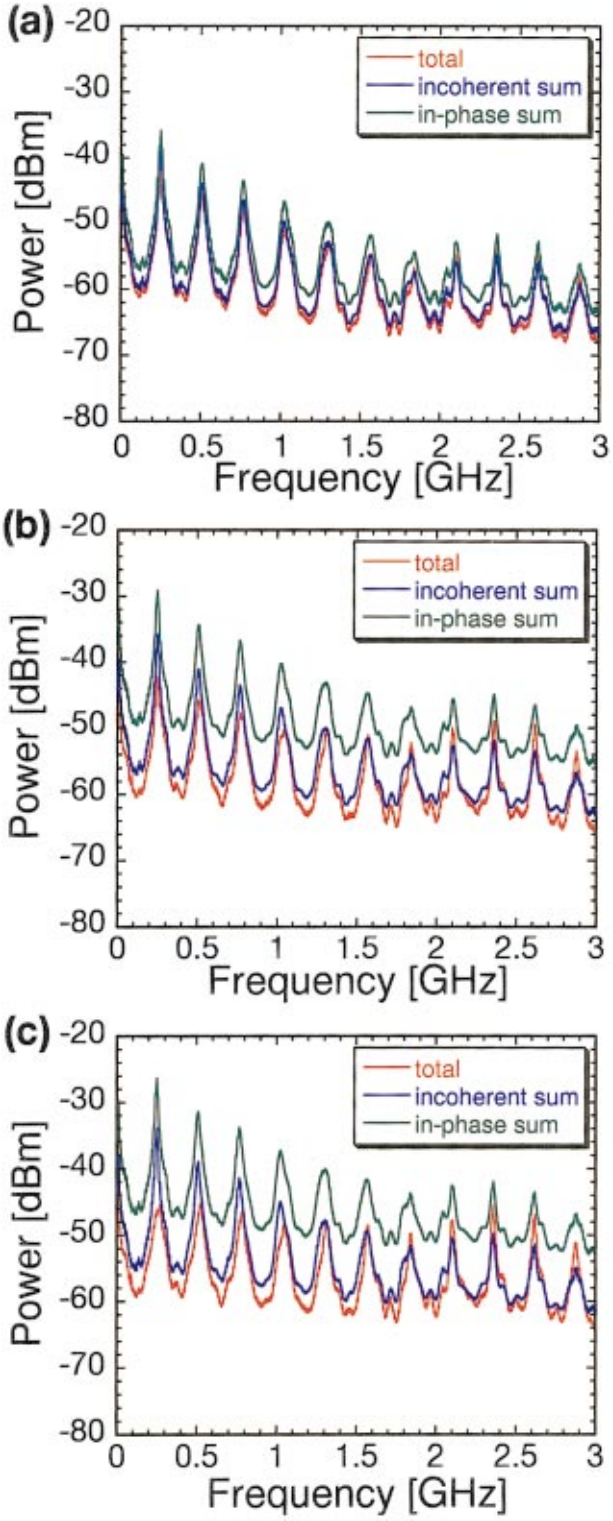

FIG. 7. (Color) Radio-frequency power spectral densities in the second laser when the first and second lasers are coupled in a master-slave scheme. The meaning of the color lines and cases (a)–(c) are the same as in Fig. 3. The phase dynamics in the second laser is synchronized with those in the first laser.

zation of the dynamics of two lasers, including the antiphase properties, is possible. Understanding the antiphase dynamics under synchronization will be important for designing new coding schemes for chaotic multiwavelength data multiplexing in an all-optical system [8,9].

Figure 5 shows the experimental setup for synchronization [7]. The output of the selected mode in the first laser is transmitted through a single-mode fiber and injected into the second semiconductor laser, which has no external mirror. Two optical isolators and an optical fiber isolator (total isolation of 90 dB) are introduced in the transmission line to guarantee the unidirectional coupling from the first laser to the second laser. A polarization controller is employed to compensate for possible polarization distortions in fiber transmission.

Figure 6 shows temporal wave forms for the total intensity of the two laser outputs before and after the synchronization. When the second laser is not matched to the first laser, the light injection has little effect on the output of the second laser and the latter shows very weak fluctuations as shown in Fig. 6(a). When two lasers are well matched through adjusting the bias injection current and the temperature of the two lasers and the injection power is appropriately set, the shape of the optical spectrum of the second laser becomes identical to that of the first laser (Fig. 2), i.e., injection locking is achieved between the two lasers. Synchronization of the oscillations of the total intensity output of the two lasers is observed under the conditions for injection locking as shown in Fig. 6(b).

Here we show that not only the wave form of total intensity but also antiphase behavior can be reproduced in the second laser. We compared a typical rf spectrum of total intensity with that of the summed intensity in the second laser with optical injection as in Fig. 3. Figure 7 shows PSD of the total and summed intensity for selected (a) three-mode, (b) ten-mode, and (c) 18-mode intensities in the second laser, respectively. Judged from the PSD spectra, thenature of the mode dynamics in the second laser is similar to those in the first laser, i.e., in-phase dynamics around the relaxation oscillation frequency and antiphase dynamics at lower frequencies. Although it is not conclusive that all the modal intensities are individually synchronized, the similarity between Figs. 3 and 7 show clearly that phase dynamics with similar frequency dependence is reproduced in the second laser by the signal injected from the first laser.

IV. CONCLUSION

We have presented clear experimental evidence that antiphase dynamics occurs in a multimode semiconductor laser with optical feedback. Specifically, for fast chaotic oscillations obtained with weak optical feedback, we have shown the relative phases of modal intensity oscillations over the full frequency range up to the relaxation oscillation frequency. We have shown that perfect in-phase dynamics of modal intensities appears at the relaxation oscillation frequency ($\sim$2.4 GHz), while partial antiphase dynamics occurs at lower frequencies. This behavior becomes more evident with the increase of the number of longitudinal modes. We have also shown that the antiphase dynamics can be reproduced in a second laser which is synchronized to the first by optical injection.

ACKNOWLEDGMENTS

We gratefully acknowledge stimulating discussions with K. Otsuka and P. Mandel, and we thank B. Komiyama for encouragement and support at ATR.

[1] G. Huyet, S. Balle, M. Giudici, C. Green, G. Giacomelli, and J.R. Tredicce, Opt. Commun. **149**, 341 (1998).
[2] G. Vaschenko, M. Giudici, J.J. Rocca, C.S. Menoni, J.R. Tredicce, and S. Balle, Phys. Rev. Lett. **25**, 5536 (1998).
[3] E.A. Viktorov and P. Mandel, Phys. Rev. Lett. **85**, 3157 (2000).
[4] F. Rogister, P. Mégret, O. Deparis, and M. Blondel, Phys. Rev. A **62**, 061803(R) (2000).
[5] D.W. Sukow, T. Heil, I. Fischer, A. Gavrielides, A. Hohl-AbiChedid, and W. Elsäßer, Phys. Rev. A **60**, 667 (1999).
[6] G. Huyet, J.K. White, A.J. Kent, S.P. Hegarty, J.V. Moloney, and J.G. McInerney, Phys. Rev. A **60**, 1534 (1999).
[7] I. Fischer, Y. Liu, and P. Davis, Phys. Rev. A **62**, 011801 (2000).
[8] J.K. White and J.V. Moloney, Phys. Rev. A **59**, 2422 (1999).
[9] Y. Liu, P. Davis, and T. Aida, IEEE J. Quantum Electron **37**, 337 (2001).
[10] P. Mandel, ''*Theoretical Problems in Cavity Nonlinear Optics* (Cambridge University Press, Cambridge, 1997).
[11] K. Otsuka, *Nonlinear Dynamics in Optical Complex Systems* (KTK Scientific Publishers, Tokyo, 1999).
[12] K. Otsuka, P. Mandel, M. Georgiou, and C. Etrich, Jpn. J. Appl. Phys., Part 2 **32**, L318 (1993).
[13] B.A. Nguyen and P. Mandel, Opt. Commun. **112**, 235 (1994).
[14] K. Wiesenfeld, C. Bracikowski, G. James, and R. Roy, Phys. Rev. Lett. **65**, 1749 (1990).
[15] M.A. Larotonda, A.M. Yacomotti, and O.E. Martinez, Opt. Commun. **169**, 149 (1999).
[16] P. Khandokhin, Y. Khanin, Y. Mamaev, N. Milovsky, E. Shirokov, S. Bielawski, D. Derozier, and P. Glorieux, Quantum Semiclassic. Opt. **10**, 97 (1998).
[17] V.A. Gorobets, K.V. Kozlov, B.F. Kuntsevich, and V.O. Petukhov, Kvant. Elektron. (Moscow) **27**, 21 (1999) [Quantum Electron. **29**, 303 (1999)].
[18] P. Mandel, B.A. Nguyen, and K. Otsuka, Quantum Semiclassic. Opt. **9**, 365 (1997).